HOLOS
ISSN 1807 - 1600

NONLINEAR NUMERICAL ANALYSIS OF FOUR PILE-CAP USING CONCRETE DAMAGED PLASTICITY

R.S. SPOZITO, F.M. ALMEIDA FILHO, R.G. DELALIBERA, A.L. CHRISTOFORO
Instituto Federal de Educação, Ciência e Tecnologia de São Paulo
ORCID: https://orcid.org/0000-0003-0509-5232
rspozito@ifsp.edu.br

Submitted June 5, 2023 - Accepted December, 2025

DOI: 10pts.15628/holos.2025.15871

ABSTRACT

The CDP (Concrete Damaged Plasticity) is a constitutive relation used for numerical simulation of reinforced concrete elements. The technical literature does not present discussions about use of these methodologies in piles-caps. This study analyzed the behavior of numerical models of four pile-caps with the CDP. A parameterization of the CDP variables was performed for calibrating the models and analyzing the structural behavior. Considering the processing methodologies, the quasi-static model presented less computational effort, however, it is recommended that its use be carried out with a refined mesh in the order of 3% of the smallest dimension of the volumetric element. Furthermore, the values of the CDP parameters result different considering the methodology of process, requiring calibration through parameterizations for different type of processing.

KEYWORDS: calibration, concrete damaged plasticity, pile-caps, reinforcement concrete.

ANÁLISE NÃO LINEAR DE BLOCOS DE CONCRETO SOBRE 4 ESTACAS UTILIZANDO A RELAÇÃO CONSTITUTIVA *CONCRETE DAMAGED PLASTICITY*

RESUMO

O CDP (*Concrete Damaged Plasticity*) é uma relação constitutiva utilizada para simulação numérica de elementos de concreto armado. A literatura técnica não apresenta discussões sobre o uso destas metodologias em blocos de concreto sobre estacas. Este estudo analisou o comportamento de modelos numéricos de blocos de concreto sobre 4 estacas com o CDP. Foi realizado uma parametrização das variáveis do CDP para calibração dos modelos e análise do comportamento estrutural. Considerando as metodologias de processamento, o modelo quasi-static apresentou menor esforço computacional, no entanto, recomenda-se que seu uso seja efetuado com uma malha refinada na ordem de 3% da menor dimensão do elemento volumétrico. Além disso, os valores dos parâmetros do CDP não foram coincidentes entre os solucionadores, necessitando realizar a calibração por meio de parametrizações para diferentes modos de processamento.

Palavras-chave: blocos de concreto sobre estacas, calibração, concreto armado, concrete damaged plasticity

1 INTRODUCTION

Pile-Caps are foundation elements with purpose transferring the forces of the structure to the foundations and are, in general, buried, which makes their visual inspection difficult.

ABNT NBR 6118 (2014), ACI 318:19 (2019), CEB-FIC 2010 (2012) recommend the use of strut-and-tie method (STM) for the design of pile caps, however, there is no consensus between the methodologies. In addition, ABNT NBR 6118 (2014) allows the use of non-linear numerical models to evaluate the performance of the reinforced concrete structure, being an auxiliary tool in structural projects. For this, the results of the numerical models must present reliability in the simulation of the mechanical behavior.

The use of numerical models for simulating 4 pile-caps proved to be feasible (IYER & SAM, 1992; Nogueira & Souza, 2006), resulting a methodology used with aim understanding the mechanical behavior of these elements (Bloodworth et al., 2012; Meléndez et al., 2016) and in proposition of sizing models (Meléndez et al., 2019).

The CDP (Concrete Damage Plasticity) is a constitutive model based on the Drucker-Prager criterion, which consists of a multiaxial model for simulating reinforced concrete elements, wich demonstrated good results in nonlinear analysis of reinforced concrete structures (Milligan et al. , 2020; Panahi & Genikomsou, 2022; Silva et al., 2021), however, as contextualized by Silva, Christoforo and Carvalho (2021), despite its feasibility, the parameter values in the CDP model does not has consensus in the literature.

Szczecina and Winnicki (2016) contextualizes the use of the CDP model allows obtaining realistic results, even for D-Regions. Alfarah; Lopez-Almansa; Oller (2017) contextualizes that the model presents good results for situations of uniaxial and biaxial stress of concrete, not recommending its use for cases of significant triaxial stresses, however, the authors do not clearly describe this limitation.

The analysis of reinforced concrete elements using the CDP constitutive relation occurred in structural elements such as beams (Aktas & Sumer, 2014), shear walls (Husain et al., 2019; Pelletier & Léger, 2017) and slabs (Milligan et al.; Nguyen et al., 2019; Panahi & Genikomsou, 2022). The technical literature does not clearly present the use of CDP for analyzing the mechanical behavior of four pile-caps, as well as the feasibility of using solvers for processing numerical models of these elements.

Being a multiaxial constitutive model that associates the models of damage and plasticity of concrete, the understanding use of CDP in volumetric elements with different solvers contributes to structural design area, since use of these methodologies become an auxiliary tool for analysis of structural behavior, in addition to contributing for future research be more careful.

In this study, the measurement of numerical models was carried out using the constitutive relation CDP and different solvers of experimental models present in the literature with differences type of failure, disposition of reinforcement and geometry of the column, associating the mechanical behavior of the experimental models with numerical models.

2 BIBLIOGRAFIC REVIEW

Sam and Iyer (1995) analyzed the feasibility of numerical models for the simulation the structural behavior of four pile-caps, with satisfactory results for prediction failure in order of 88% of experimental models analyzed, indicating feasibility of numerical models.

Nogueira and Souza (2006) also evaluated use of numerical models with experimental results from Sam and Iyer (1995) in the DIANA program, however, the authors indicate use of several constitutive models which allowed the prediction of failure forces in 90 % of experimental results.

Souza et al (2007) used the plastic fracture model based on the formulation of scattered cracks (CC3NonLinCementitious2) from the DIANA program library. The authors analyzed mechanical behavior through curves of forces and displacements between the numerical and experimental models of campaign by Suzuki, Otsuki and Tsubata (1998) (BP-20-30, BPC-20-30, BP-30-25, BPC-30-25, BP-30-30, BPC-30-30). Authors estimated the failure force with numerical models in the order of 90%, except for the BPC-20-30 model, with an estimate of 76%.

Still using the DIANA program, Bloodworth, Cao and Xu (2012) simulated mechanical behavior of four pile caps with one column dimension equal to cap dimension. The reliability analysis of numerical model was based on cracking pattern and ultimate force, in addition to identifying the compressive stress flow that described strut shape.

Meléndez, Miguel and Pallarés (2016), through numerical models discretized in the computational program FESCA 3D, identified the importance of considering the tensile strength of concrete to predict the ultimate strength. The authors analyzed models from campaign by Suzuki et al (1998) resulting, depending on the parameterization of constitutive models, predictions with a variation of 0.8 to 1.22 the failure force of the experimental models.

In literature, there are also studies using numerical models to simulate mechanical behavior of pile cap with two, three and six piles. For two-pile cap Ansys® was used in several studies (Delalibera et al., 2014; Delalibera & Sousa, 2021; Gonçalves et al., 2022), in case three-pile cap the ATENA 3D program was used (Buttignol & Almeida, 2013) and, in case of six-pile cap was used software DIANA (Oliveira et al., 2014).

Despite the numerical models results satisfactory predictions of rupture force, it identify that the studies do not present the use of the CDP relation together with solvers, as well as the discussion of results in relation to the methodology used for numerical simulation.

HOLOS
ISSN 1807 - 1600

3 CDP CONSTITUTIVE MODEL

CDP model combines the principles of plasticity and damage, that is, the model is expressed considering plastic behavior of the material (irreversible) and stiffness degradation due to microcracks.

The plasticity parameters required by CDP are the dilation angle (ψ), eccentricity (ϵ), relation of biaxial and uniaxial resistances (σ_{bo}/σ_{co}), the fault surface in the deviation plane normally to the hydrostatic axis (K_c) and the viscosity parameter (μ).

Considering necessity to define stiffness degradation of elements, the damaged values for compression (d_c) and tension (d_t) must be indicate. The damage is calculated as a function of the ratio of stress in the material for a given deformation (σ_c or σ_t) by compressive strength of concrete (f_c) and for tensile strength (f_{ct}) (Systèmes, 2013).

The values for the parameters of dilation angle (ψ), biaxial and uniaxial stress ratio (σ_{bo}/σ_{co}), deviation plane ratio (K_c) and viscosity coefficient (μ) were defined according to the survey carried out in the study by Silva, Christoforo and Carvalho (2021), indicated in Table 1, adopting the most common values in the technical literature.

Table 1 Interval of values adopted in the CDP parameterization.

Parameters	$\boldsymbol{\psi}$	$\boldsymbol{\epsilon}$	$\boldsymbol{\sigma_b/\sigma_c}$	$\boldsymbol{K_c}$	$\boldsymbol{\mu}$
Interval	13º - 55º	0.1	1.16 – 1.75	0.667 – 0.700	1E-3, 1E-4 e 1E-5

4 ABAQUS® PROGRAM SOLVERS

Abaqus® has solvers described as ABAQUS/Standard and ABAQUS/Explicit. Both solvers can be used with CDP. ABAQUS/Explicit has characteristic of non-linear explicit dynamic formulation for analysis of systems requested by dynamic and quasi-static loads, obtaining the material deformation by difference between increments.

The Abaqus/Standard solver presents characteristic of static solver with viscoplastic regularization, defined by viscosity parameter (μ). Due to model convergence, it may present processing errors for complex geometries, and presents a higher computational cost when compared to ABAQUS/Explicit.

Although ABAQUS/Explicit solver has advantage in terms of computational cost, the criteria of low values of kinetic energy in system must be monitored for results are reliable (Systèmes, 2013). The studies of Nguyen, Tan and Kanda (2019) and Earij et al. (2017) used the ABAQUS/Explicit solver with the constitutive relation CDP.

For ABAQUS/Explicit mode, in this study, the simulations were performed using "double precision" criterion with a displacement applied with a 0.25 mm/s.

5 METHODOLOGY

The characteristics of materials in reference models are presented in Table 2, according to tests carried out by the authors. The specimens are referenced with the acronym M4EY, where "Y" indicates the experimental model analyzed, equal "A" for the model by Chan and Poh (2000) and "B" for specimen BPC-30-30 of Suzuki et al. (1998). The combination of CDP parameters is identified by a two-digit numeral in front of the M4EY abbreviation, with only the results of processed models being indicated.

Table 2 Characteristics of experimental models

			Concrete						Steel				
			Cap				Column and Piles						
Model		F_{exp} **(kN)**	f_c (MPa)	f_{ct} (MPa)	E_c (MPa)	μ	E_c (MPa)	μ	$A_{s,T}$ (cm²)	f_y (MPa)	f_u (MPa)	μ (MPa)	**Es (MPa)**
Pile Cap A	M4EA	1230	31,76	2,49	31.116,22	0,20	37.277,87	0,20	6,28	480,70	552,00	0,30	200GPa
BPC 30-30	M4EB	1034	30,09	2,36	30.606,90				5,70	405,00	592,00		

The tensile strength and modulus of elasticity of concrete were obtained using the recommendations of Eurocode 2 (CEN, 2004) with $f_{ct} = 0{,}3.f_c^{2/3}$ and $E_c = 22.[f_c/10]^{0,3}$. The compressive strength value of the concrete (f_c) was defined based on the results of the respective authors. The material of the column and the piles have higher resistance values to present a greater rigidity in relation to the behavior of the cap.

The dimensions of the analyzed models are indicated in Figure 1. The strut inclination angles, obtained using the model by Blévot and Frémy (1967), have values equal to 42.59º for the specimen of Chan and Poh (2000) (Pile Cap A) and 45.29º for the specimen of Suzuki et al (1998) (BPC 30-30).

HOLOS
ISSN 1807 - 1600

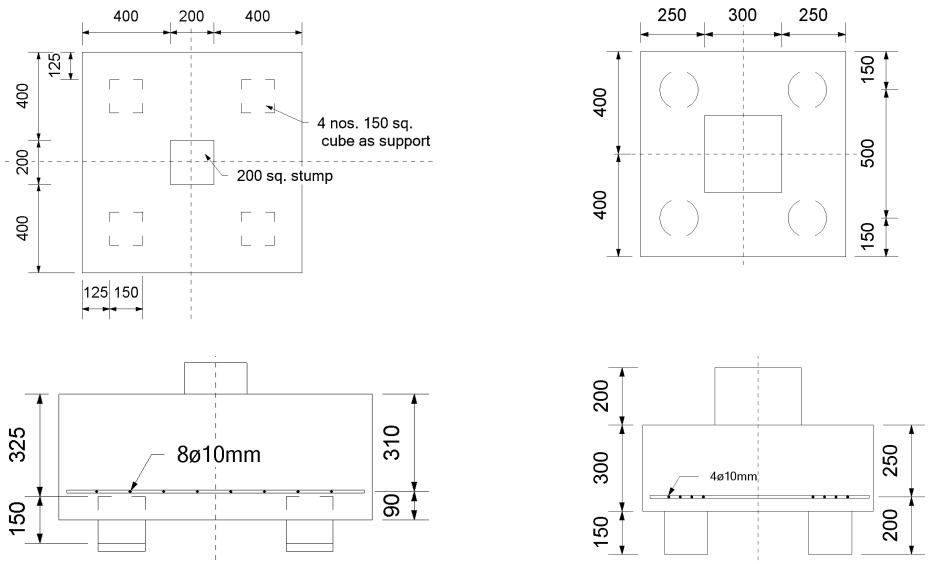

Figure 1 Specimens of (a) Chan and Poh (2000) and (b) Suzuki et al (1998)

The loading of the numerical models was done with the application of uniformly distributed displacements over the top of column. The elements adopted to simulate behavior of concrete were C3D8R (8-node volumetric) and the T3D2 (two-node linear) for reinforcement. The connection of the T3D2 elements with the C3D8R elements was carried out with embedded Abaqus® command.

The connection between the lower face of the column and the upper face of the supports with the block was Tie type. In the case of the M4EA model, the only model that has embedded supports (piles), it was decided to use a contact interface with a coefficient of friction equal to 0.3 (Friction Penalty) and restriction to the normal displacement of the surfaces of the Hardening type. For the ABAQUS/Explicit solver, the friction between the lateral face of the piles and the pile cap was discarded because it is a limitation of the processing mode.

The uniaxial force and deformation curve of concrete, necessary for the CDP, was obtained with the constitutive model of Carreira and Chu (1985). To define the stress and strain curve, based on the considerations indicated by Systèmes (2013) who describe mesh sensitivity effects when there is no reinforcement in significant regions of the model, a fracture energy model was used, in accordance with what is presented in the literature. technique using this methodology (Milligan et al., 2020; Nana et al., 2017; Panahi & Genikomsou, 2022).

The value of fracture energy (G_F) is related to the concrete compressive strength (f_c) (Equation 1), according to Model Code 1990 (1993). G_{fo} was obtained through an interpolation of values as a function of the maximum aggregate size (d_{max}), as proposed by Nana et al (2017)

(Equation 2). The proposal of Model Code 2010 (2012) resulted in a resistance behavior much higher than expected, similarly obtained in study of Nana et al (2017). The value adopted for the aggregate diameter (d_{max}) was equal to 10 mm.

$$G_F = G_{fo}.(f_c/10)^{0.7} \quad (1)$$

$$G_{fo} = (0.00005\, d_{max}^2 - 0.0005\, d_{max} + 0.026) \quad (2)$$

For steel, the behavior represented by a bilinear diagram with a linear elastic stretch and a plasticity threshold (Earls, 1999) was adopted, obtained according to the characteristics of the materials presented in Table 1. The M4EA and M4EB models are illustrated in Figure 2. The mesh size for both models was defined according to the study carried out for both solvers that are discussed in a specific topic in this study.

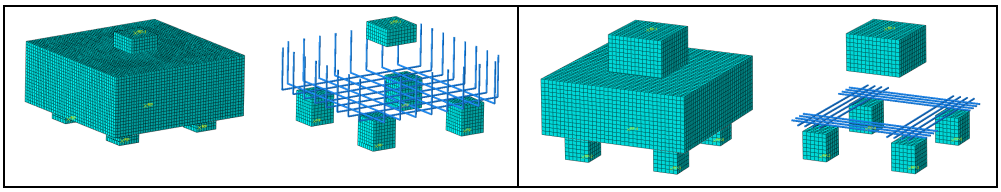

(a) (b)

Figure 2 Modelos (a) M4EA e (b) com detalhes de malha e armadura

The methodology for calibrating the force and displacement curve was realized with the processing of models with the parameterization of the value of ψ and, from the best convergence curve, the processing of models with the parameterization of values of σ_b/σ_c and K_c was carried out. Finally, the parameterization of the value of μ for the ABAQUS/Standard mode was done, since the ABAQUS/Explicit solver does not use the convergence criteria by viscosity.

To assessment the CDP model with the Abaqus® solvers, initially the results of the force and displacement curve between the numerical and experimental models were analyzed and, based on the results of better agreement with the experimental model, the analysis between numerical model was realized considering the solvers.

The computer used has an Intel I7-11800H processor, 16Gb of RAM memory, SSD hard disk with 1TB capacity and NVidia 3060TI video card with 4GB.

HOLOS
ISSN 1807 - 1600

6 RESULTS AND DISCUSSIONS

6.1 Specimen of Chan e Pho (2000) – M4EA

6.1.1 Mesh Study

Figure 3 illustrates the result of force and displacement curves as a function of mesh size. The number of discretized finite elements for pile-cap with 20mm mesh was 48,976 and in the case of the 15mm mesh, a total of 115,612 elements were obtained. Based on these results, the use of 20mm mesh was defined for process of calibration the force and displacement curve for both solvers, minimizing the computational effort.

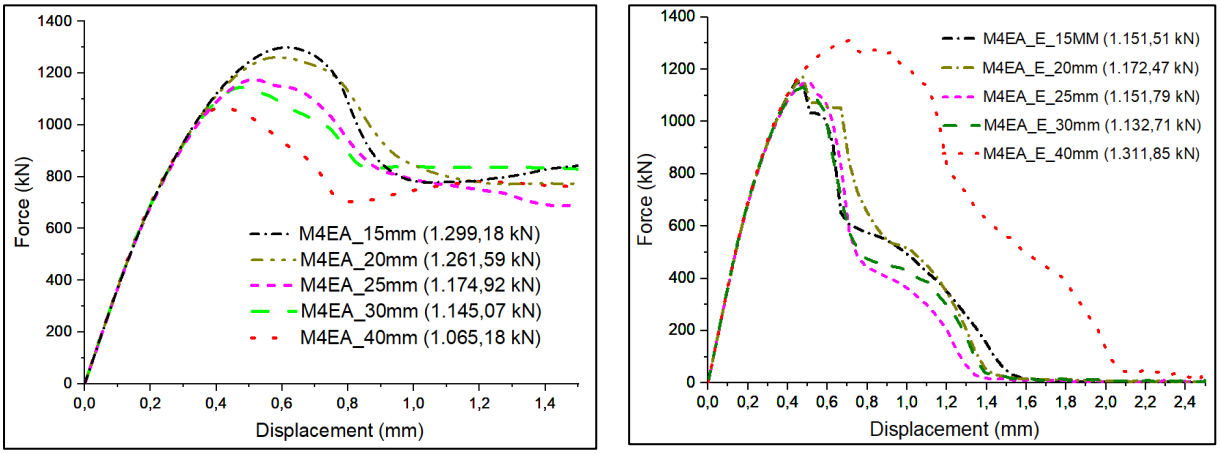

(a) (b)

Figure 3 Force and displacement curves for (a) Standard and (b) Explicit processing modes

For the ABAQUS/Standard solver, the model with mesh size equal 20mm presented a similar behavior to the 15mm, with a difference of approximately 3% between the maximum force values, justifying its choice. In the case of the ABAQUS/Explicit mode, curves with dimensions of 25mm, 20mm and 15mm showed similar behavior.

6.1.2 Force and Displacement Curve Calibration

Chan and Poh (2000), authors of the experimental campaign of the M4EA model, described the behavior of the force and displacement curve to experimental model “Pile Cap A” with rupture force equal to 1230 kN. Up to a force of approximately 800 kN, the behavior of curve is linear with appearance of first cracks close to the described value. From 800 kN, the intensity of force

HOLOS
ISSN 1807 - 1600

increases up to 1230 kN with a displacement of 6 mm and, later, there was a decrease in the resistant force and, consequently, greater displacements. Figure 4 (“Pile Cap A”) highlights the result of the experimental model.

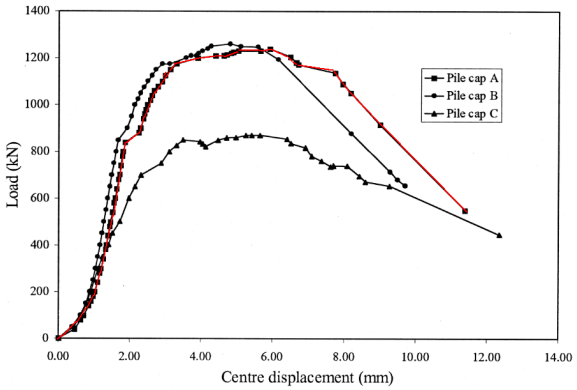

Figure 4 Highlighted curve of the PILE CAP "A" experimental model referring to the M4EA model

6.1.2.1 Solver ABAQUS/Standard

The resulted curves with parameterization of ψ are shown in Figure 5 for M4EA. It was observed that the value equal to 36º indicated better correlation with curve of experimental model.

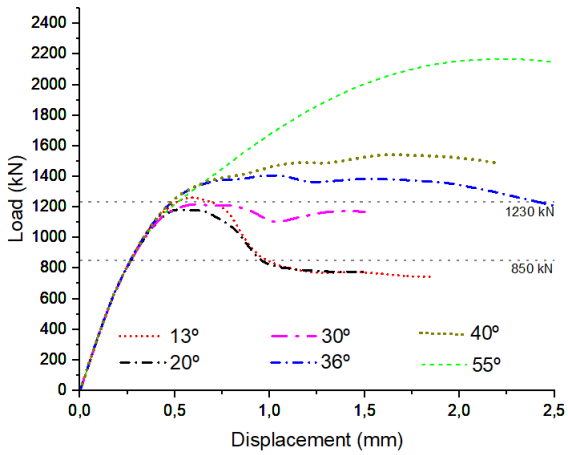

Figure 5 Force and displacement curves of the M4EA model with the parameterization of ψ

In reinforced concrete beams Earij et al (2017) identified that low ψ values result in loss of ductility of element. Nana et al (2017) contextualizes the parameter is associated with failure

mode, indicating low values produce a brittle failure behavior. That behaviors do not show similarity to associate with results obtained in simulations of four pile caps analyzed.

Nguyen et al (2019) identified that ψ is not sensitive to bending behavior, which may explain the behavior of the curve for the analyzed models, where they presented the same behavior in the initial stretches of request.

Figure 6 illustrates the force and displacement curves for ψ equal to 36º with the parameterization of σ_b/σ_c and K_c. The models were processed with the parameter μ equal to 1E-5 and 1E-4 in Figure 6.a and Figure 6.b, respectively. The ϵ parameter has a value equal to 0.1 for all models.

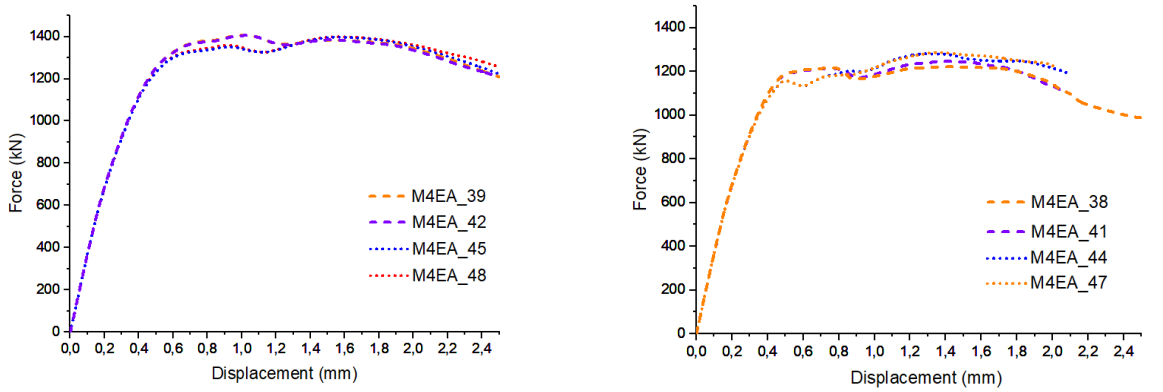

M4EA39: $\sigma_c/\sigma_b = 1.16, K_c = 0.667$ M4EA45: $\sigma_c/\sigma_b = 1.75, K_c = 0.667$
M4EA42: $\sigma_c/\sigma_b = 1.16, K_c = 0.700$ M4EA48: $\sigma_c/\sigma_b = 1.75, K_c = 0.700$

(a)

M4EA38: $\sigma_c/\sigma_b = 1.16, K_c = 0.667$ M4EA44: $\sigma_c/\sigma_b = 1.75, K_c = 0.667$
M4EA41: $\sigma_c/\sigma_b = 1.16, K_c = 0.700$ M4EA47: $\sigma_c/\sigma_b = 1.75, K_c = 0.700$

(b)

Figure 6 Force and displacement graph of parameterization the σ_b/σ_c and K_c for μ equal to (a) 1E-3 and (b) 1E-4

In Figure 6.a and Figure 6.b, changing the K_c parameter did not significantly influence the results of the force and displacement curves. In the case of the parameter σσ_c/σ_b, there was an interference in the behavior of the curve, mainly for the models in Figure 6.b, which have the value of μ equal to 1E-4. Increasing the value of σ_c/σ_b alters the failure surface of the CDP model, which may explain the strength gain for models processed with σ_c/σ_b equal to 1.75.

The influence of the discussed parameters was not significant in changing the maximum force value of the models. Thus, the values of the parameters σ_c/σ_b and K_c for the simulation of the elements of this study were adopted as suggested by Systèmes (2013), equal to 1.16 and 0.667, respectively.

The displacements of numerical models showed greater stiffness compared to experimental model. The force and displacement curve obtained with ψ equal to 36º required a scale adjustment to represent behavior of experimental model (Figure 7).

HOLOS
ISSN 1807 - 1600

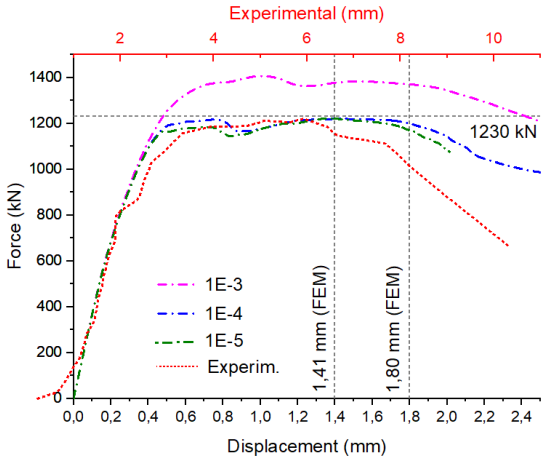

Figure 7 Force and displacement curves for numerical and experimental M4EA model.

Figure 7 also presents the parameterization curves for the value of μ, and it is possible to observe that the numerical models processed with values equal to 1E-4 and 1E-5 have similar behavior. The models presented a maximum displacement force equal to 1.41mm, of 1,221 kN and, from the displacement of 1.80mm, the numerical models result in a decrease force, like experimental model.

Table 4 presents the numerical models and their respective values of the CDP parameters, the results of maximum forces and displacement obtained in the curve and the relationship between the numerical and experimental models. The percentage column indicates the resistance gain value in relation to the curves with μ equal to 1E-5 of the grouped values.

Table 3 Maximum forces of ABAQUS/Standard numerical models (ϵ = 0.1)

				M4EA $F_{exp} = 1230\ kN$			
Modelo	σ_c/σ_b	**Kc**	**μ**	F_{CDP} **(kN)**	↑ (%)	**(mm)**	$\frac{F_{CDP}}{F_{exp}}$
M4EA _37	1.16	0.667	1E-5	1220.61	-	1,39	0.992
M4EA _38			1E-4	1221.84	0.10	1,43	0.993
M4EA _39			1E-3	1406.81	15.25	1.02	1.143
M4EA_40		0.700	1E-5	1241.27	-	1.34	1.009
M4EA _41			1E-4	1245.59	1.40	1.41	1.012
M4EA _42			1E-3	1405.07	13.56	1.02	1.142
M4EA_43	1.75	0.667	1E-5	1279.80	-	1.38	1.040
M4EA _44			1E-4	1281.00	0.09	1.29	1.041
M4EA _45			1E-3	1397.88	9.23	1.57	1.136

Modelo	σ_c/σ_b	Kc	μ	M4EA $F_{exp} = 1230\ kN$ F_{CDP} (kN)	↑ (%)	(mm)	$\frac{F_{CDP}}{F_{exp}}$
M4EA _47		0.700	1E-4	1286.27	-	1.37	1.045
M4EA _48			1E-3	1399.35	-	1.57	1.137

The M4EA_37 model was selected for analyzes using the CDP and the ABAQUS/Standard solver, since the model presented a value closer to the ultimate load of the experimental model. Despite this approximation, the model also showed greater stiffness (Figure 7) to displacements. This behavior is discussed in the technical literature for concrete blocks on 2 piles (Luchesi et al., 2022).

6.1.2.2 Solver ABAQUS/Explicit

All curves with a 20mm mesh showed maximum values close to the rupture value of the experimental model. The model with ψ equal to 55º showed the maximum value of the numerical model with the greatest displacement, and the behavior was analyzed with the parameterization of $\sigma_c/\sigma_b$and K_c (Figure 8.b).

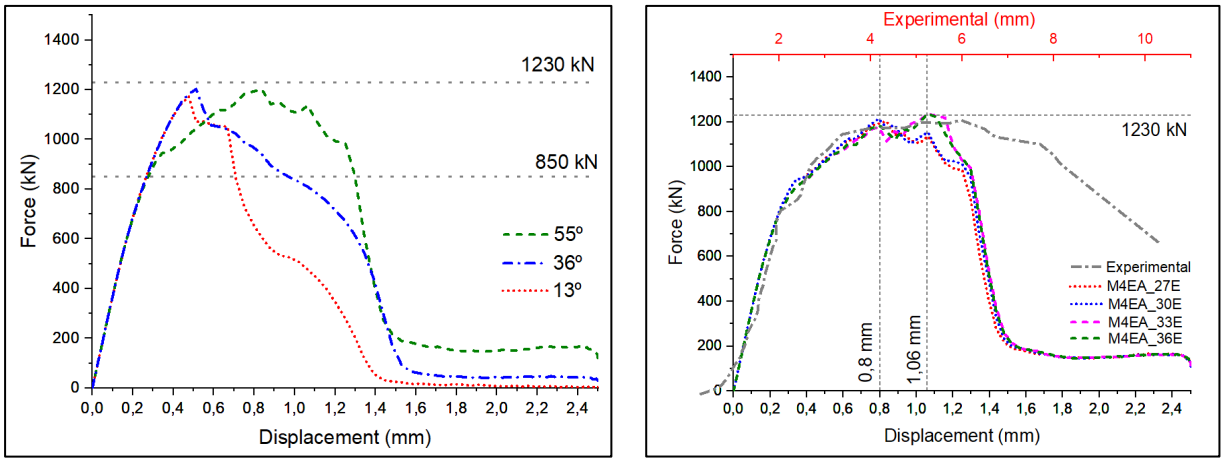

(a) (b)

Figure 8 Parameterization with ABAQUS/Explicit of parameters (a) ψ and (b) $\sigma_c/\sigma_b$and K_c

HOLOS
ISSN 1807 - 1600

The results of the parameterization of σ_c/σ_b and K_c (Figure 8.b) showed similar characteristics to ABAQUS/Standard solver, and with the change from 1.16 to 1.75 of σ_c/σ_b, the curves indicated resistance gains of approximately 8,5%, higher when compared to the ABAQUS/Standard methodology, which resulted in gains of around 5%.

Considering the failure mode of the element characterized by the displacement gain without an increase in ultimate force, it was decided to process models with a refined mesh (10 mm) with the objective of better simulating the structural behavior, requiring a new calibration of ψ (Figure 9). The result indicated that the refined mesh represented the force and displacement curve with greater similarity to the experimental model, but without benefits regarding displacement.

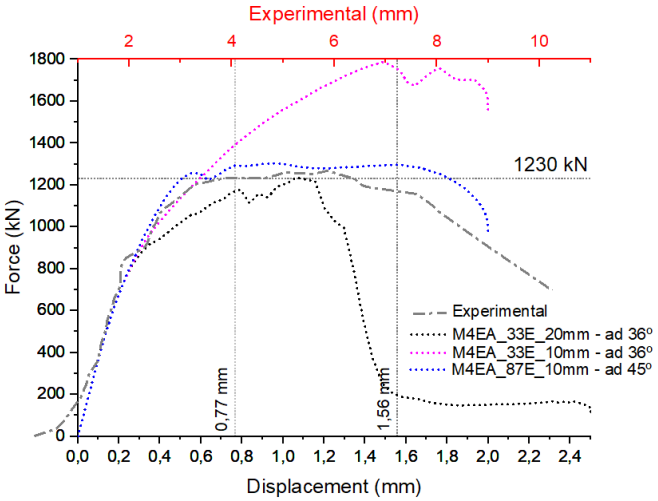

Figure 9 Force and displacement graph of the ABAQUS/Explicit model for 10mm mesh

The calibration of force and displacement curves was performed only with ψ values, which indicated an influence on the behavior only after the initial stretch for the ABAQUS/Explicit mode, because first calibration did not reach satisfactory results in behavior of the curve. For the 10 mm models, the analysis of the parameterization of σ_c/σ_b and K_c was not carried out due to the curve presenting results with good convergence, resulting in ψ equal to 45º (M4EA_87E). Table 5 indicates the maximum values of the forces obtained for the models processed with the ABAQUS/Explicit solver.

Table 4 Maximum force of ABAQUS/Explicit numerical and experimental models

					$F_{exp} = 1230\ kN$			
Model	ψ	ϵ	σ_c/σ_b	**Kc**	F_{CDP} **(kN)**	↑ (%)	**(mm)**	$\frac{F_{CDP}}{F_{exp}}$
20mm								
M4EA_27E	55	0.1	1.16	0.667	1202.79	-	0.84	0.977
M4EA_30E				0.700	1213.29	0.87	0.79	0.986
M4EA_33E			1.75	0.667	1235.55	-	1.06	1.004
M4EA_36E				0.700	1237.81	0.18	1.06	1.006
10mm								
M4EA_33E	55	0.1	1.16	0.667	1788.65	-	1.49	1.450
M4EA_87E	45	0.1	1.16	0.667	1298.89	-	1.56	1.055

In Abaqus/Explicit mode the ultimate force value with the value of σ_c/σ_b equal to 1.75 was 2.72% higher, in the case of parameterization of K_c the increase was 0.87% for the value of σ_c/σ_b equal to 1.16. This behavior also allows proposing for modeling with the Abaqus/Explicit solver to use values suggested in Systèmes (2013), like the ABAQUS/Standard mode.

6.1.2.3 Computacional cost

Model processing times are indicated in Figure 10.

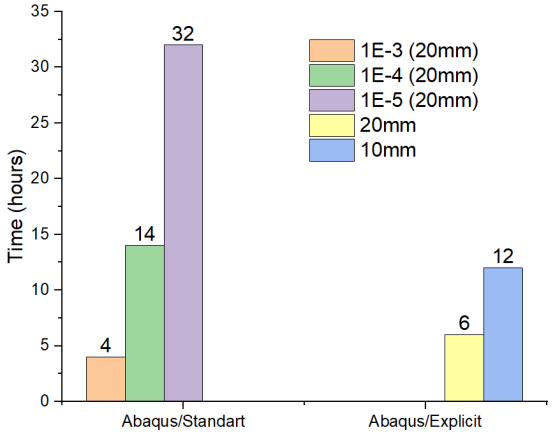

Figure 10 Average processing time of numerical models

HOLOS
ISSN 1807 - 1600

For the ABAQUS/Standard solver, the value of μ significantly influenced the computational cost. From the results obtained in the numerical models processed, the value of μ equal to 1E-3 presented more conservative results when compared to models processed with 1E-4 and 1E-5. Furthermore, values of μ equal to 1E-5 are suggested to obtain similar results for processing models with solvers discussed in this work for other structural elements (Genikomsou & Polak, 2015). In this study, there was a compatibility between the curves equal to 1E-5 and 1E-4, therefore suggesting maximum values of the viscosity parameter equal to 1E-4.

Regarding the computational cost, it is possible to observe that the model processed with ABAQUS/Explicit obtained an average time shorter than the models processed with ABAQUS/Standard with μ equal to 1E-4 and a more refined mesh, resulting in a methodology with a lower computational cost and similar results for the analysis of concrete blocks on 4 piles.

6.1.3 Compressive stresses and concrete degradation

The stress flow analysis was associated with the scalar degradation of the concrete, expressed by the SDEG variables, resulting from the combination of tensile (DAMAGET) and compression (DAMAGEC) damage variables. The analysis was performed on a section obtained by cutting at 45º in the pile cap, passing through two piles in models M4EA_37, M4EA_33E and M4EA_87E.

In the processing time with higher resistive strength of the M4EA_37 and M4EA_87E models (Figure 11), the damage associated with the concrete resulted in the splitting of the compressive stress flow. In the case of model M4EA_33E, this behavior was not verified. Concrete degradation was more influenced by tensile damage (DAMAGET).

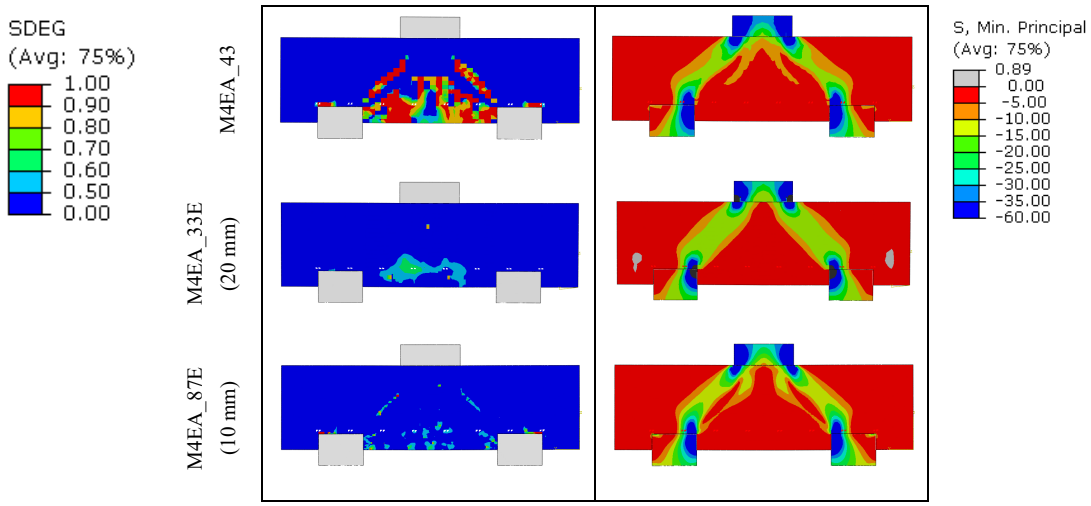

Figure 11 Degradação da rigidez e tensões de compressão

Figure 12 illustrates values of DAMAGET variable at instant of maximum force value for models M4EA_37, M4EA_33E and M4EA_87E. The M4EA_87E model obtained a more concentrated tensile degradation of concrete in the lower part of the compressive stress flow when compared to the M4EA_37 model.

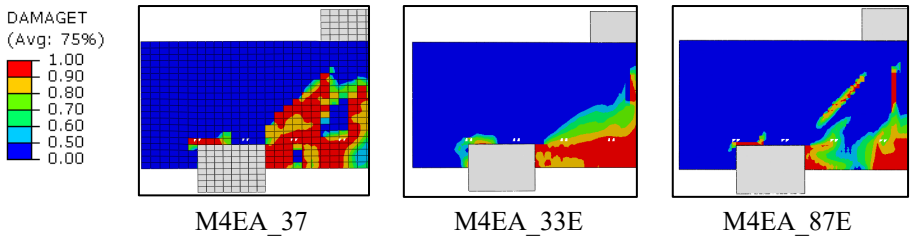

Figure 12 Dano do concreto à tração para os modelos de processamento no instante de maior valor da força.

The results of studies allow identifying the occurrence of stress concentration on the upper face of the piles for two-pile cap (Delalibera & Giongo, 2008), four-pile cap (Buttignol & Almeida, 2013) and six-pile cap (Oliveira et al., 2014). The results of the numerical models obtained for the M4EA showed similarity, however, the M4EB did not present this characteristic. This behavior can be related to the rigidity of the supports, as identified in the study by Meléndez, Miguel and Pallarés (2016).

Figure 13.a and Figure 13.b illustrate the stress flows in the model with displacement equal to 1.45 mm (F = 1221 kN) and 1.80 mm (F = 1201 kN), respectively, for the M4EA_37 model. Figure 13.c and Figure 13.d highlight the stress envelopes with values above 10 MPa, detailing the stress concentration at the supports. For the M4E_33E model, the results were similar, with the stress concentration in the pile.

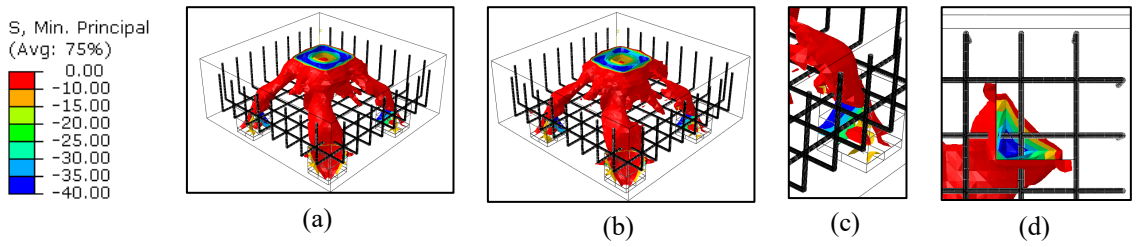

Figure 13 Fluxos de tensões principais de compressão para o modelo M4EA_37

Figure 14 illustrates the stress flow behavior of the M4EA_87E model. The processing times refer to displacement of 0.78 mm (F=1293 kN - Figure 14.a) and 1.57 mm (F=1298 kN - Figure 14.b), after this displacement, the connecting rod also presented its uncharacterized shape, as M4EA_37. The behavior occurred similarly for the stress concentration in the pile (Figure 14.c Figure 14.d).

Another feature is that at a displacement of 0.78 mm there was no tension request above 10MPa in the connecting rod, with this feature at the end of the plateau of the force and displacement curve.

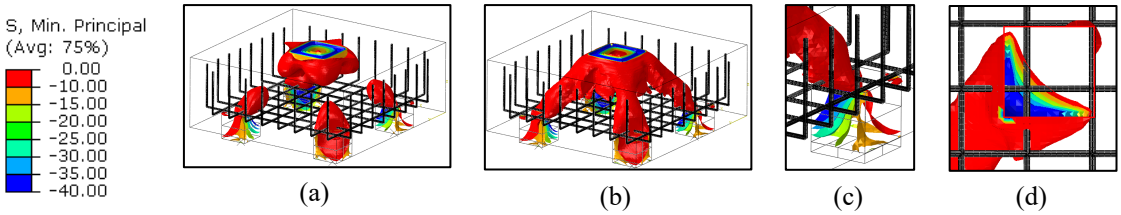

Figure 14 Compressive principal stress flows for model M4EA_87E

The behavior of models M4EA_37 and M4EA_87E are similar for stress flow and values of maximum resistant capacity, it is not possible to identify the behavior for the model M4EA_33E. Thus, it is possible to identify that the calibration of the model only by the value of the ultimate force of the experimental model can result in a different mechanical behavior, being also dependent on the solvers used, and the mesh criteria defined.

6.1.4 Stress in reinforcements

Chan and Poh (2000) described the reinforcements reached yielding values at the moment of maximum loading. The authors do not clearly indicate the values obtained as a function of the arrangement of the strain gauges. Figure 15 illustrates the stresses obtained in the models and the location of strain gauges in experimental program.

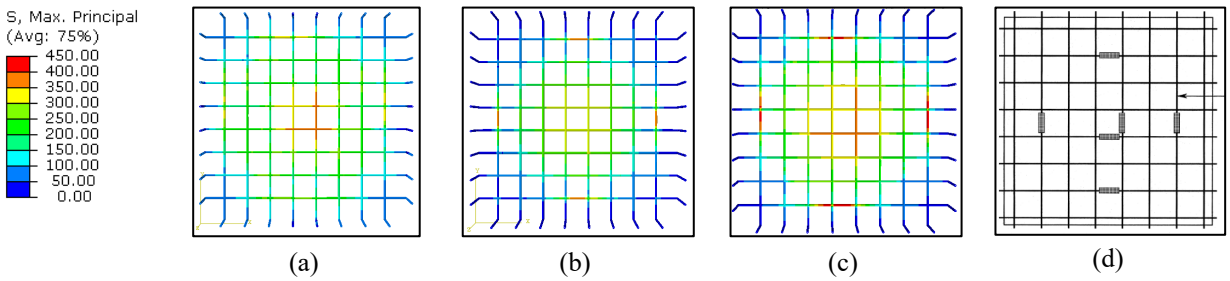

Figure 15 Tensile stress (MPa) of the reinforcements of the model (a) M4EA_37, (b) M4EA_33E and (c) M4EA_87E and (d) extensometers of the experimental model

The model best represented the stress behavior of reinforcements was M4EA_87E, with values in the order of 425 MPa, however, these values are obtained in the lateral reinforcements

of cap. At the points with strain gauges installed, numerical models showed similar behavior, but with even greater values in the M4EA_87E model.

6.1.1 Cracking pattern of models

Chan and Poh (2000) illustrated the cracking pattern of the model and, in analysis of models M4EA_43, M4EA_33E and M4EA_87E, they showed a similar pattern of cracking (Figure 16), that is, with diagonal cracks between the piles.

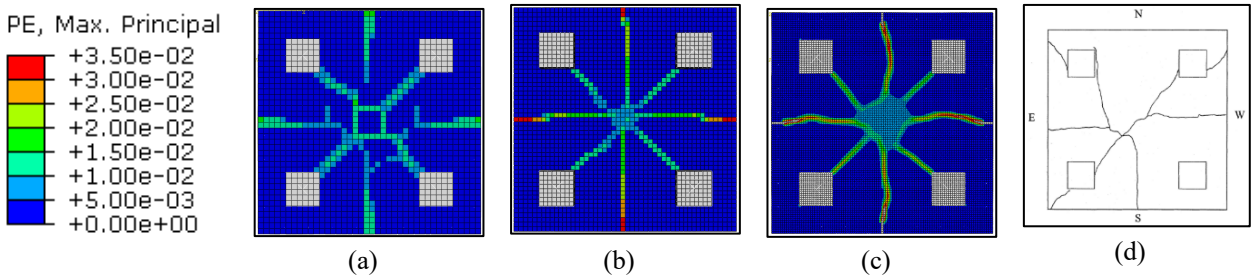

Figure 16 Cracking pattern on the underside of the model (a) M4EA_37, (b) M4EA_33E and (c) M4EA_87E

Cracking on the underside of the numerical model was best represented by model M4EA_87E. Despite the convergence of the cracking pattern, the models did not capture the cracking on the lateral face of the blocks, and arch cracks were not represented in the numerical models. This behavior may be related to the rigidity that the numerical models presented.

6.2 Model Suzuki, Otsuki and Tsubata (1998) – M4EB

The mesh study carried out for the M4EB showed a difference of approximately 6% between the 15 mm and 20 mm models for the ABAQUS/Standard mode, adopting the value of 20 mm. For the Abaqus/Explicit mode, it was also verified the need to adopt a 10 mm mesh, according to the M4EA model.

6.2.1 Force and Displacement Curve Calibration

Suzuki, Otsuki e Tsubata (1998), autores do programa experimental do modelo M4EB, descrevem que a ruptura do modelo ocorreu em função dos esforços de cisalhamento com uma

ruptura frágil, posterior a falha da flexão, ou seja, após a região do gráfico de ganho de deslocamentos sem aumento da força resistente.

The experimental curve of processing the M4EB numerical models is illustrated in Figure 17 together with the curve obtained by the experimental campaign and by the numerical modeling by Souza et al (2007). The ABAQUS/Explicit mode calibration of the force and displacement curve resulted in the mesh being divided by 10mm and a ψ equal to 50º (M4EB_99E).

The M4EB_33E, using the parameter values obtained for the M4EA, resulted in 25% lower of the ultimate force when compared to the experimental model. The M4E_99E curve obtained good convergence with the experimental result, with a characteristic of a significant drop in the carrying capacity of the numerical model in the displacement close to that obtained by the experimental model.

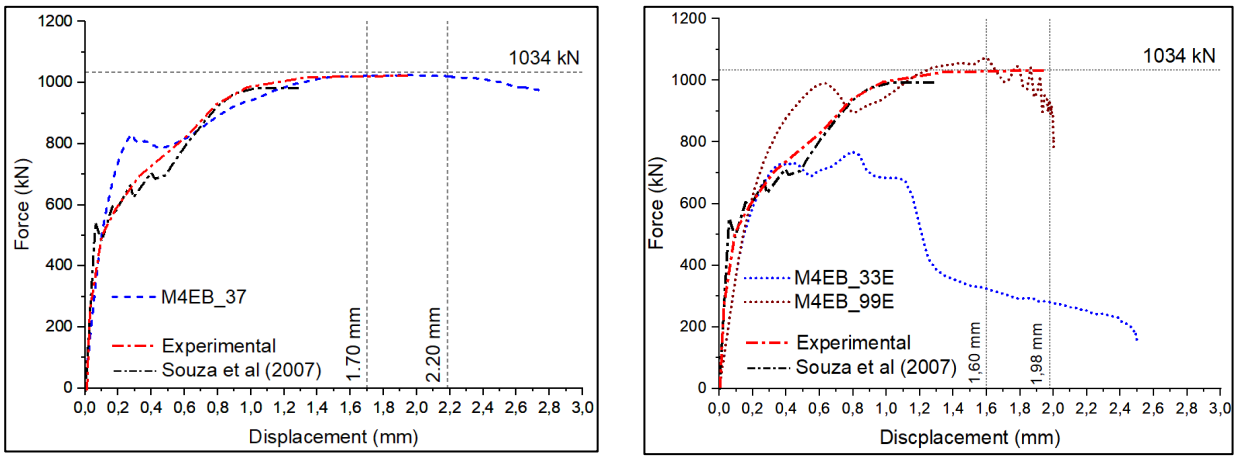

Figure 17 M4EB force and displacement curves for (a) Abaqus/Standard and (b) ABAQUS/Explicit mode

Table 5 summarizes the values obtained in the processed models and other author.

Table 5 Strengths of the numerical and experimental models of the M4EB

Model	ψ	ϵ	σ_c/σ_b'	Kc	μ	Mesh size (mm)	F (kN)	(mm)	$\frac{F}{F_{exp}}$
Experimental	-	-	-	-	-	-	1034.00*	~ 2.00	1.000
Souza et al (2007)	-	-	-	-	-	-	951.90	~1.00	0.920
M4EB _37	36	0.1	1.16	0.667	1E-5	20	1024.82	1.70	0.992
M4EB_33E	36	0.1	1.16	0.667	-	20	768,80	0.79	0.743
M4EB_99E	50	0.1	1.16	0.667	-	10	1071.61	1.60	1.036

Model	ψ	ϵ	σ_c/σ_b'	Kc	μ	Mesh size (mm)	F (kN)	(mm)	$\frac{F}{F_{exp}}$
* Average value of two specimens from the experimental campaign									

It was identified that constitutive relation CDP, for both solvers used in Abaqus®, presented satisfactory results for the M4EB, however, the use of equal parameters between the solvers does not converge to similar results for models discretized in similar ways, that is, with mesh size and values of the CDP parameters.

6.2.2 Compressive stresses and concrete degradation

Figure 18 illustrates the associated concrete damage values and stress flow in the 45° section passing through two piles with displacements of 1.70 mm and 2.20 mm from M4EB_37. Like M4EA model, the combination for determination of scalar degradation (SDEG) occurred with predominance of tensile damage.

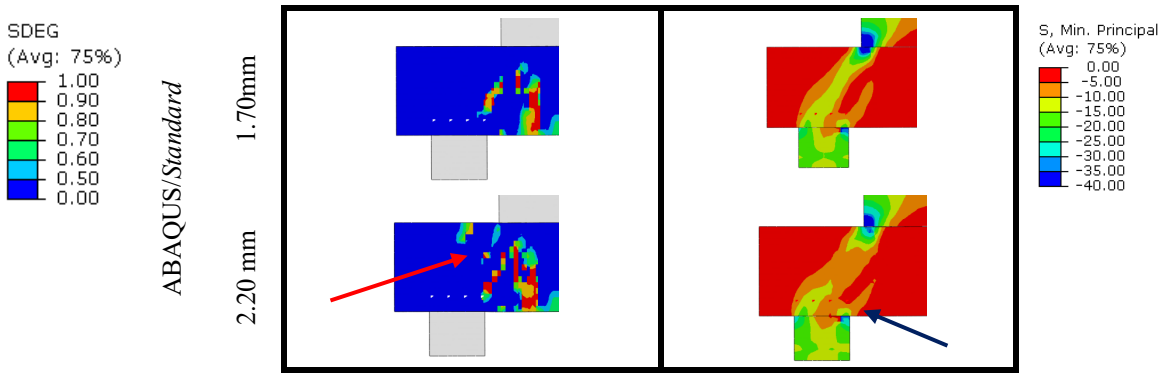

Figure 18 Concrete degradation (SDEG) and compressive stress flow of model M4EB_37

For the M4E_99E model, with the same section for analysis (Figure 19), the stress flow was presented differently when compared to the M4EB_37 model. Stresses of greater value, between 10 and 15 MPa, have, considering their longitudinal axis, a more centralized direction in relation to the upper face of the piles at the level of reinforcement. Regarding degradation associated with concrete (SDEG), the model M4EB_99E showed values of greater predominance below 0.50.

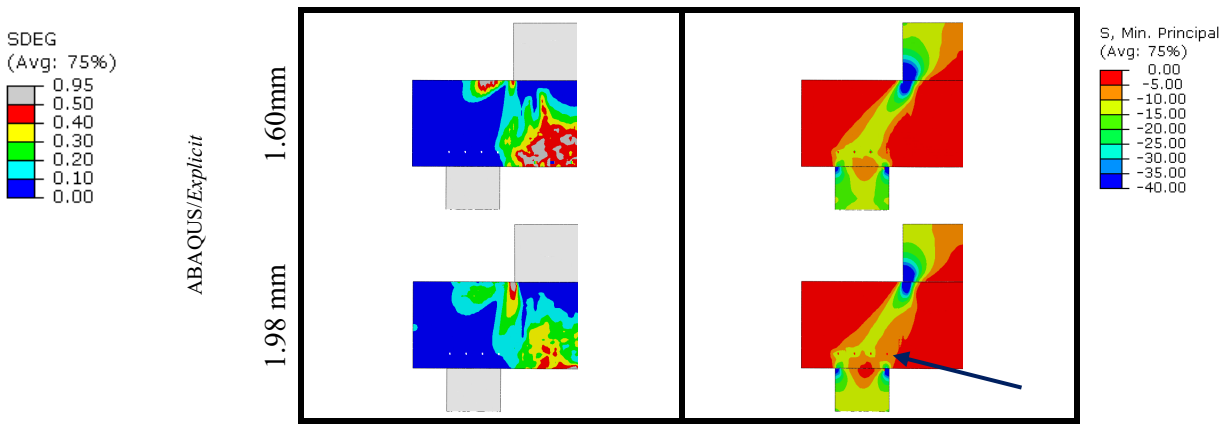

Figure 19 Concrete degradation (SDEG) and compressive stress flow of model M4EB_99E

Both models (M4EB_37 and M4EB_99E) showed a stress drop (indicated by the stress envelope) after the maximum force value in the region highlighted by an arrow (Figure 18 and Figure 19), above the top face of the pile and below line of the reinforcement, behavior like that obtained in the results of numerical models by Meléndez et al (2019).

6.2.1 Stress in reinforcements

Reinforcement stress values are illustrated in Figure 20 at processing time of greatest resisting force of the numerical models.

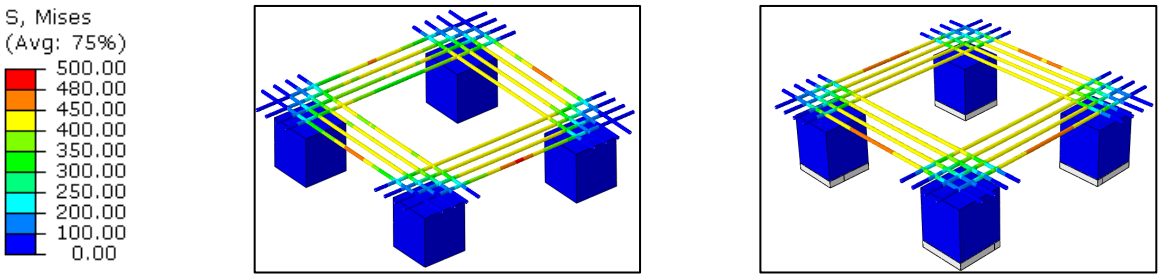

Figure 20 Reinforcement tensile stress of numerical models (a) M4EB_37 and (b) M4EB_99E

The reinforcements of M4EB_37 result values close to yielding. For the M4EB_99E model, the reinforcement loads were like those obtained by the M4EB_37 model, with a slightly higher value. Suzuki et al (1998) did not measure the deformation of the reinforcement. Regarding the behavior between numerical models with different solvers, the results were similar for reinforcement requests.

6.2.2 Cracking pattern of models

Suzuki et al. (1998) obtained a failure behavior by shear, characterized by cracks around piles. This failure, associated with the cracking pattern of the experimental models, were similar in numerical models, as illustrated in Figure 21, with greater evidence for model M4E_99E.

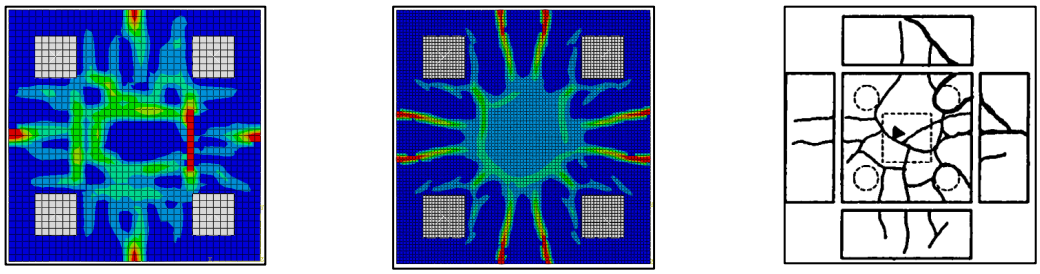

(a) (b) (c)

Figure 21 Cracking pattern of models (a) M4EB_37, (b) M4EB_99E, and (c) Experimental

The M4EB_99E model showed better cracking convergence. This result indicates a good relationship between the ABAQUS/Explicit solver and the experimental model. Noteworthy that simplification of the pile to a square section did not present significant differences in results, however, a more refined analysis is suggested for this simplification in relation to the localized failure modes.

7 Conclusions

Based on the obtained results, it can be concluded that:

1. The CDP model was viable for simulating the behavior of concrete blocks on 4 piles, allowing the evaluation of the mechanical behavior of the elements analyzed for both Abaqus® solvers.
2. Identical values assigned to the CDP parameters do not result in similar behavior between numerical models for solvers.
3. The results obtained by the ABAQUS/Explicit solver using CDP obtained a good relationship with the experimental models and, considering the minimization of the computational effort, the use of this methodology proved to be a viable tool for simulating the behavior of concrete blocks on 4 piles.
4. The support stiffness influenced the results of displacements and stress concentration on the upper face of the supports (piles) of the M4EA model. For the M4EB model, the

displacement was compatible, without the occurrence of stress concentration in the supports (piles), requiring investigations on the discretization of the supports.

As the main result of this study, it was possible to identify that the use of the constitutive relation CDP is feasible for the simulation of concrete block elements on 4 piles. In addition, it was also possible to identify that both solvers discussed in the work were also viable for the analysis of the mechanical behavior of these elements, however, the calibration of the parameters must be performed for each solver.

Regarding the CDP variables, the results indicated that the values of K_c and σ_b/σ_c can be defined with values equal to 1.16 and 0.667, respectively, as suggested by Systèmes (2013). Regarding the ψ parameter, values can range from 36º to 50º, depending on the adopted solver. Finally, it is suggested for the Abaqus/Explicit mode, the mesh size has order of 3% of the smallest dimension of the volumetric element.

8 REFERÊNCIAS

Aktas, M., & Sumer, Y. (2014). Nonlinear finite element analysis of damaged and strengthened reinforced concrete beams. *Journal of Civil Engineering and Management*, *20*(2), 201–210. https://doi.org/10.3846/13923730.2013.801889

Alfarah, B., López-Almansa, F., & Oller, S. (2017). New methodology for calculating damage variables evolution in Plastic Damage Model for RC structures. *Engineering Structures*, *132*, 70–86. https://doi.org/10.1016/j.engstruct.2016.11.022

AMERICAN CONCRETE INSTITUTE. ACI 318-19: Building code requirements for structural concrete. (2019). An ACI Standard. *ACI Committee 318*.

Associação Brasileira de Normas Técnicas. (2014). NBR 6118 - Projeto de Estruturas de concreto - Procedimento. *Associação Brasileira de Normas Técnicas*, 238.

Blévot, J., & Frémy, R. (1967). *Annales de l'Institut Technique du Batiment et des Travaux Publics*.

Bloodworth, A. G., Cao, J., & Xu, M. (2012). Numerical Modeling of Shear Behavior of Reinforced Concrete Pile Caps. *Journal of Structural Engineering*, *138*(6), 708–717. https://doi.org/10.1061/(asce)st.1943-541x.0000499

Buttignol, T. E. T., & Almeida, L. C. (2013). Concrete compressive characteristic strength analysis of pile caps with three piles. *Revista IBRACON de Estruturas e Materiais*, *6*(1), 158–177. https://doi.org/10.1590/s1983-41952013000100009

Carreira, D. J., & Kuang-Han Chu. (1985). Stress-Strain Relatonship for Reinforced Concrete in Compression. *ACI Structural Journal*, *November-December*, 797–804.

CEB-FIP C. (1993). Model Code 1990 for Concrete Structures, Comit e Euro-International du Beton and Federation Internationale de la Precontrainte. In *FIB bulletin* (p. 105). London: Thomas Telford.

CEB-FIP C. (2012). *Model Code 2010-Final draft: Volume 1: fib Federation internationale du beton;*

Chan, T. K., & Poh, C. K. (2000). Behaviour of precast reinforced concrete pile caps. *Construction and Building Materials*.

COMITÉ EUROPÉEN DE NORMALISATION. (2004). *Eurocode 2: Design of concrete structures – Part 1–1: General rules and rules for buildings; 1*(2005).

Delalibera, R. G., Da Silva, W. A., & Giongo, J. S. (2014). Análise numérica de blocos sobre duas estacas com cálice embutido submetido à ação de força horizontal. *Ciencia y Engenharia/ Science and Engineering Journal*, *23*(1), 83–91. https://doi.org/10.14393/19834071.2014.26852

Delalibera, R. G., & Giongo, J. S. (2008). Deformações nas diagonais comprimidas em blocos sobre duas estacas. *Revista IBRACON de Estruturas e Materiais*, *1*(2), 121–157. https://doi.org/10.1590/s1983-41952008000200002

Delalibera, R. G., & Sousa, G. F. (2021). Numerical analyses of two-pile caps considering lateral friction between the piles and soil. *Revista IBRACON de Estruturas e Materiais*, *14*(6), 1–19. https://doi.org/10.1590/s1983-41952021000600004

Earij, A., Alfano, G., Cashell, K., & Zhou, X. (2017). Nonlinear three–dimensional finite–element modelling of reinforced–concrete beams: Computational challenges and experimental validation. *Engineering Failure Analysis*, *82*(March), 92–115. https://doi.org/10.1016/j.engfailanal.2017.08.025

Earls, C. J. (1999). Effects of material property stratification and residual stresses on single angle flexural ductility. *Journal of Constructional Steel Research*, *51*(2), 147–175. https://doi.org/10.1016/S0143-974X(99)00024-3

Genikomsou, A. S., & Polak, M. A. (2015). Finite element analysis of punching shear of concrete slabs using damaged plasticity model in ABAQUS. *Engineering Structures*, *98*, 38–48. https://doi.org/10.1016/j.engstruct.2015.04.016

Gonçalves, V. F., Delalibera, R. G., & de Oliveira Filho, M. A. (2022). Analysis of the pile-to-cap connection of pile caps on two steel piles – An experimental and numerical study. *Engineering Structures*, *252*(July 2021). https://doi.org/10.1016/j.engstruct.2021.113629

Husain, M., Eisa, A. S., & Hegazy, M. M. (2019). Strengthening of reinforced concrete shear walls with openings using carbon fiber-reinforced polymers. *International Journal of Advanced Structural Engineering*, *11*(2), 129–150. https://doi.org/10.1007/s40091-019-0216-6

IYER, P. K., & SAM, C. (1992). THREE-DIMENSIONAL ANALYSIS OF PILE CAPS. *Compurers & Srrucrwes*, *42*(3), 395–411.

Luchesi, G. L., Randi, R. de P., Trautwein, L. M., & Almeida, L. C. de. (2022). Important aspects in experimental versus numerical comparative analysis in pile caps. *Revista IBRACON de Estruturas e Materiais*, *15*(5), 1–16. https://doi.org/10.1590/s1983-41952022000500002

Meléndez, C., Miguel, P. F., & Pallarés, L. (2016). A simplified approach for the ultimate limit state analysis of three-dimensional reinforced concrete elements. *Engineering Structures*, *123*,

330–340. https://doi.org/10.1016/j.engstruct.2016.05.039

Meléndez, C., Sagaseta, J., Miguel, P. F., & Rubio, L. P. (2019). Refined three-dimensional strut-and-tie model for analysis and design of four-pile caps. *ACI Structural Journal*, *116*(4), 15–29. https://doi.org/10.14359/51714485

Milligan, G. J., Polak, M. A., & Zurell, C. (2020). Finite element analysis of punching shear behaviour of concrete slabs supported on rectangular columns. *Engineering Structures*, *224*(October 2019), 111189. https://doi.org/10.1016/j.engstruct.2020.111189

Nana, W. S. A., Bui, T. T., Limam, A., & Abouri, S. (2017). Experimental and Numerical Modelling of Shear Behaviour of Full-scale RC Slabs Under Concentrated Loads. *Structures*, *10*, 96–116. https://doi.org/10.1016/j.istruc.2017.02.004

Nguyen, T. N. H., Tan, K. H., & Kanda, T. (2019). Investigations on web-shear behavior of deep precast, prestressed concrete hollow core slabs. *Engineering Structures*, *183*(January), 579–593. https://doi.org/10.1016/j.engstruct.2018.12.052

Nogueira, T. B., & Souza, R. A. de. (2006). Análise, dimensionamento e verificaçao de elementos espaciais em concreto armado utilizando o método dos elementos finitos e o método das bielas. *Revista Internacional de Metodos Numericos Para Calculo y Diseno En Ingenieria*, *22*(1), 31–44.

Oliveira, D. S., Barros, R., & Giongo, J. S. (2014). Blocos de concreto armado sobre seis estacas: simulação numérica e dimensionamento pelo método de bielas e tirantes. *Revista IBRACON de Estruturas e Materiais*, *7*(1), 1–23. https://doi.org/10.1590/s1983-41952014000100002

Panahi, H., & Genikomsou, A. S. (2022). Comparative evaluation of concrete constitutive models in non-linear finite element simulations of slabs with different flexural reinforcement ratios. *Engineering Structures*, *252*(August 2021), 113617. https://doi.org/10.1016/j.engstruct.2021.113617

Pelletier, K., & Léger, P. (2017). Nonlinear seismic modeling of reinforced concrete cores including torsion. *Engineering Structures*, *136*, 380–392. https://doi.org/10.1016/j.engstruct.2017.01.042

Sam, C., & Iyer, P. K. (1995). Nonlinear finite element analysis of reinforced concrete four-pile caps. *Computers and Structures*, *57*(4), 605–622. https://doi.org/10.1016/0045-7949(95)00068-R

Silva, L. M. E., Christoforo, A. L., & Carvalho, R. C. (2021). Calibration of concrete damaged plasticity model parameters for shear walls. *Revista Materia*, *26*(1). https://doi.org/10.1590/s1517-707620210001.1244

Souza, R. A., Kuchma, D. A., Park, J., & Bittencourt, T. N. (2007). Nonlinear Finite Element Analysis of Four-Pile Caps Supporting Columns Subjected To Generic Loading. *Computers and Concrete*, *4*(5), 363–367.

Suzuki, K. ., Otsuki, K. ., & Tsubata, T. (1998). Influence of Bar Arrangement on Ultimate Strength of Four-Pile Caps. *Transactions of the Japan Concrete Institute*, *20*, 195–202.

Systèmes, D. (2013). *ABAQUS ANALYSYS USER´s MANUAL*.

Szczecina, M., & Winnicki, A. (2016). Selected Aspects of Computer Modeling of Reinforced Concrete Structures. *Archives of Civil Engineering*, *62*(1), 51–64. https://doi.org/10.1515/ace-2015-0051

COMO CITAR ESTE ARTIGO:
Saverio Spozito, R., Almeida Filho, F. M. de, Delalibera, R. G., & Christoforo, A. L. . Análise não linear de blocos de concreto sobre 4 estacas utilizando a relação constitutiva Concrete Damaged Plasticity . HOLOS, 5(41). https://doi.org/10.15628/holos.2025.15871

SOBRE OS AUTORES

RAPHAEL SAVERIO SPOZITO, IFSP - Instituto Federal de São Paulo
Graduado em Engenharia Civil pela Faculdade de Engenharia de Ilha Solteira (2005), especialização em Engenharia de Softwares e Banco de Dados pela Universidade Estadual de Londrina (2009) e Engenharia de Segurança do Trabalho pela Faculdade União dos Grandes Lagos (2014), mestrado em Engenharia Civil pela Universidade Estadual Paulista "Júlio de Mesquita Filho" (2017), atualmente é doutorando no Programa de Pós-Graduação em Engenharia Civil na Universidade de São Carlos na área de Estruturas com tema de pesquisa em blocos de concreto sobre estacas. É professor de Ensino Básico, Técnico e Tecnológico no Instituto Federal de Educação, Ciência e Tecnologia de São Paulo desde 2014.
E-mail: rspozito@ifsp.edu.br
ORCID: https://orcid.org/0000-0003-0509-5232

FERNANDO MENEZES DE ALMEIDA FILHO, Universidade Federal de São Carlos (UFSCar)
Graduado em Engenharia Civil pela Universidade Federal do Ceará (1998), especialização em Engenharia de Estruturas pela Universidade de Fortaleza (2000), mestrado em Engenharia de Estruturas pela Universidade de São Paulo - SET/EESC/USP (2002), doutorado em Engenharia de Estruturas pela Universidade de São Paulo - SET/EESC/USP (2006) e pós-doutorado em Engenharia de Estruturas pela Universidade de São Paulo - SET/EESC/USP (2010). Foi engenheiro do laboratório NETPre - Núcleo de Estudos e Tecnologia em Pré-moldados de concreto na UFSCar no período de 2009 a 2011 realizando diversas atividades de ensaios, projetos de pesquisa e extensão. Atualmente, é professor do curso de engenharia civil da Universidade Federal de São Carlos com ênfase em Estruturas de Concreto, atuando principalmente nos seguintes temas: Estruturas em concreto armado e protendido, análise experimental, aderência aço-concreto, mecânica das estruturas e simulações numéricas. Ainda, como linhas de pesquisa de interesse, destacam-se: Estruturas de pontes e estrutura de edifícios altos.
E-mail: almeidafilho@ufscar.br
ORCID: https://orcid.org/0000-0002-6927-6377

RODRIGO GUSTAVO DELALIBERA, Universidade Federal de Uberlândia
Graduado em Engenharia Civil para Faculdade de Engenharia de São Jose do Rio Preto (1999), Mestre em Engenharia Civil (Área de Estruturas) pela Universidade de São Paulo (2002), doutorado em Engenharia Civil (Área de Estruturas) pela Universidade de São Paulo (2006) e Pós-Doutorado em Engenharia Civil (Área de Estruturas) pela Universidade de São Paulo (2009). Atualmente é Professor Associado III na Universidade Federal de Uberlândia e diretor regional do Instituto Brasileiro de Concreto (IBRACON). Possui experiência em Engenharia Civil, com ênfase em Estruturas de Concreto, atuando nas áreas: blocos sobre estacas, concreto armado e protendido, fundações, análises numéricas e experimentais. É professor no curso de Mestrado em Engenharia Civil com linha de pesquisa em blocos de concreto sobre estacas.
E-mail: delalibera@ufu.br

ORCID: https://orcid.org/0000-0003-4730-6018

ANDRÉ LUIS CHRISTOFORO, Universidade Federal de São Carlos (UFSCar)
Graduado em Engenharia Civil pela Universidade de Franca (2000), mestre em Engenharia de Estruturas pela Universidade de São Paulo - SET/EESC/USP (2003), doutorado em Engenharia de Estruturas pela Universidade de São Paulo - SET/EESC/USP (2007) e pós-doutorado em Engenharia de Estruturas pela Universidade de São Paulo - SET/EESC/USP (2013). Atualmente é docente na Universidade Federal de São Carlos (UFSCar).
E-mail: cristoforoal@yahoo.com.br
ORCID: https://orcid.org/0000-0002-4066-080X

Editora Responsável: Francinaide de Lima Silva Nascimento

Recibido 05 de janeiro de 2023
Aceito: 1 de dezembro de 2025
Publicado: 23 de dezembro de 2025